Model predictive control simulation, implementation and performance assessment of a coal comminution circuit

E.J. Meyer[a,b], M.C. Olivier[c], L. Matumba[d], I.K. Craig[b,*]

[a] *Senior Modelling and Simulation Engineer, Product Development, UCB Pharma S.A., Chemin du Foriest 1, 1420 Braine-l'Alleud, Belgium*
[b] *Department of Electrical, Electronic and Computer Engineering, University of Pretoria, Pretoria 0002, South Africa*
[c] *Lead Control and Analytics Engineer, GE's Digital Mine, GE Corporate Park, Unit 3, 130 Gazelle Avenue, Midrand, 1683, Gauteng, South Africa*
[d] *Senior Metallurgical Engineer, Process Development, Grootegeluk Coal Mine, Lephalale, 0555, South Africa*

Abstract

This paper describes the simulation, implementation and performance assessment of model predictive control (MPC) for a coal communition circuit, and describes, as far as can be ascertained, the first implementation of MPC in the coal processing industry.

Dynamic models of an actual coal comminution circuit were derived in previous publications using the principle of mass conservation with unknown parameters that were identified with actual plant production data. The identified dynamic models are used in nonlinear MPC simulations to determine the process control objectives and to calculate a potential process improvement in throughput. This increase in potential throughput was estimated to be 5% and was used as motivation in a business case to obtain funding to implement MPC on the actual plant.

After performing a tender process, General Electric was contracted to implement the MPC. The MPC was implemented successfully on the comminution system and compared to current manual plant operational performance. After evaluating the MPC through a statistical performance assessment, it was found that throughput was improved by a significant 8.22%. The methodology followed is presented in this paper and the improved production throughput motivates for further MPC technologies to be implemented at other plant operations.

Keywords: model predictive control, coal comminution, dynamic modelling, performance assessment, simulation

1. Introduction

The work described in this paper is based on Meyer (2016) which details the development of modelling and control of coal processing plants (Meyer and Craig, 2015, 2014, 2010). In particular, this paper focuses on the simulation, implementation and performance assessment of model predictive control (MPC) for a coal comminution system at one of Exxaro Resources' metallurgical coal processing plants at Grootegeluk Mine, Limpopo, South Africa. MPC has been implemented on many industrial plants (Qin and Badgwell, 2003). What makes the work described in this paper novel is that, as far as could be ascertained, it describes the first industrial implementation of MPC in the coal processing industry. It is also rare to find an industrial application of the steps described in the general control framework (see Figure 1) in the literature. Exxaro Resources selected General Electric (GE) to implement a GE Digital Mine MPC solution on their comminution plant. The comminution system consists of three areas:

- Run-of-mine (ROM) stockpiling;
- Screening, crushing and feed bin buffer; and
- Screen feed for downstream separation circuits.

*Corresponding author. Tel.: +27 12 420 2172; fax: +27 12 362 5000
Email address: ian.craig@up.ac.za (I.K. Craig)

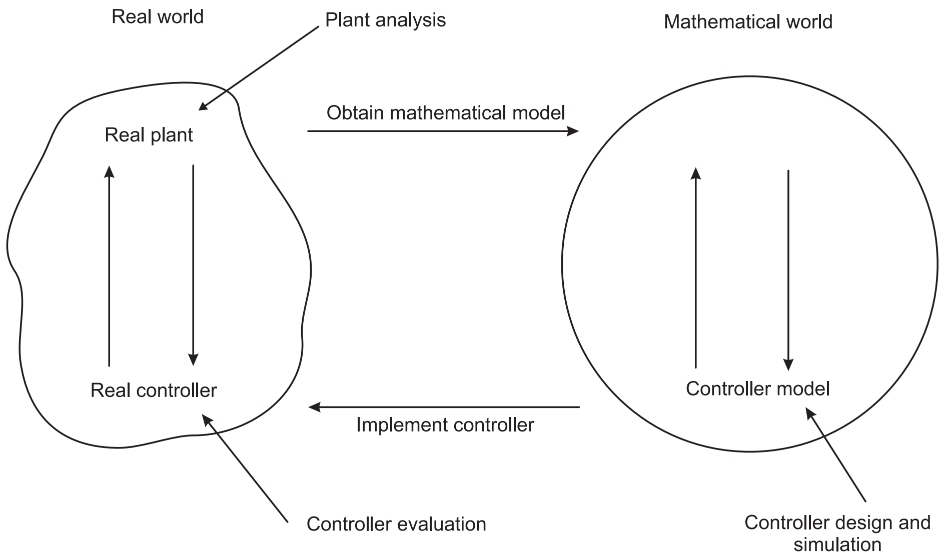

Figure 1: General control framework [taken from Craig and Henning (2000)].

The methodology of this MPC implementation follows the general control framework described in Craig and Henning (2000) and is illustrated in Figure 1. This methodology requires that a mathematical model of the real plant is developed before a control system is designed. Once the control system performs satisfactorily in simulation it is then implemented and monitored to ensure its value has been realised.

MPC (Camacho and Bordons, 2004) makes use of a dynamic model to predict future outputs based on current and past inputs and outputs. Using a reference setpoint, calculated future errors are used by an optimiser with a cost function and process constraints to determine future process inputs. Bauer and Craig (2008) shows that the process control method of choice is MPC. However, when investigating application of MPC to coal bulk material handling in available literature, most publications relate to down stream processing such as coal-fired power station and energy generation (Luo et al., 2015).

Nonlinear coal mill modelling and its application to MPC has also been shown in Cortinovis et al. (2013). The objective of the MPC was to improve energy efficiency through coordinating belt speed and feed rate or coordinating operating status and time. Open loop optimal control has also been applied to belt conveyors (Zhang and Xia, 2010, 2011). Optimal energy management for a jaw crushing process in deep mines has shown that by using a switching control technique, it is possible to reduce energy cost and consumption of a jaw crushing station (Numbi et al., 2014).

This paper demonstrates how the general control framework in Craig and Henning (2000) was followed for the simulation, implementation and performance assessment of the MPC. Initially the simulation of nonlinear MPC (NMPC) applied to a nonlinear coal comminution circuit dynamic model is given in Section 2. The dynamic model was fitted to actual plant historical data. The actual implementation of advanced process control (APC) on the real plant is described in Section 3. APC was first implemented as advanced regulatory control (ARC) (see e.g. Muller and Craig, 2016) and then as linear MPC. After having implemented APC, it was evaluated over a four-month period and compared to previous production data without APC. Section 4 details the statistical analysis showing the improvement in throughput that was actually gained when the APC was live. A conclusion of the work is presented in Section 5.

2. Nonlinear MPC simulation

MPC consists of a model that uses past and current plant values to predict future outputs. Grüne and Pannek (2011) indicate that the difference between NMPC and MPC is that NMPC makes use of a nonlinear model when applying past and current plant values to predict future outputs. Since some of the dynamic models used in this simulation are nonlinear, NMPC is used for the control simulations. The nonlinear plant is usually described by the general discrete time state space model,

$$\boldsymbol{x}_{j+1} = \boldsymbol{f}(\boldsymbol{x}_j, \boldsymbol{u}_j), \tag{1}$$

$$\boldsymbol{y}_j = \boldsymbol{g}(\boldsymbol{x}_j), \tag{2}$$

where $\boldsymbol{x}_j$ is the state vector, $\boldsymbol{y}_j$ the output vector, $\boldsymbol{f}$ and $\boldsymbol{g}$ are nonlinear functions describing the state transitions and outputs respectively, and $\boldsymbol{u}_j$ contains the input vector space.

An algorithm is used to propose future control actions based on a required reference trajectory. Using future output errors, an objective function (**J**) and process constraints, an optimiser algorithm is used to determine future inputs for the process and model (Camacho and Bordons, 2004). The objective function to be minimized may take the general form,

$$\boldsymbol{J} = \sum_{j=1}^{N} ||\hat{\boldsymbol{y}}_j - \boldsymbol{y}_s||^2_{\mathbf{R}} + \sum_{j=0}^{M-1} ||\Delta \boldsymbol{u}_j||^2_{\mathbf{P}} + \sum_{j=0}^{M-1} ||\boldsymbol{u}_j - \boldsymbol{u}_s||^2_{\mathbf{Q}} + ||\boldsymbol{s}^2_{\mathbf{T}}||, \tag{3}$$

where **P**, **Q**, **R** and **T** are weighting matrices that consider rapid input changes ($\Delta \boldsymbol{u}_j = \boldsymbol{u}_j - \boldsymbol{u}_{j-1}$), future behaviour of the input error ($\boldsymbol{u}_j - \boldsymbol{u}_s$), future behaviour of the output error ($\hat{\boldsymbol{y}}_j - \boldsymbol{y}_s$) respectively and soft constraints ($\boldsymbol{s}$). The control law (minimizing $\boldsymbol{J}$ to solve for future inputs $\boldsymbol{u}_j$) is determined over a prediction horizon (N) where $\hat{\boldsymbol{y}}$ is the output prediction and $\boldsymbol{y}_s$ is the reference trajectory. The control law is also solved for over a control horizon (M). Future input ($\boldsymbol{u}_j$) deviations from the desired steady-state inputs $\boldsymbol{u}_s$ are also controlled.

The fourth term in Equation 3 considers soft constraints on the output variables. The constraints for the process variables are usually used to restrict actuator movement ($\boldsymbol{u}_j$) and slew rate ($\boldsymbol{d}$). Typical constraints include bounds on the amplitude and slew rate of the control signals and limits on the output ($\boldsymbol{y}_j$) such as:

$$\boldsymbol{u}_{min} \leq \boldsymbol{u}_j \leq \boldsymbol{u}_{max}; \quad j = 0, 1, \ldots, M-1, \tag{4}$$

$$\boldsymbol{du}_{min} \leq \Delta \boldsymbol{u}_j \leq \boldsymbol{du}_{max}; \quad j = 0, 1, \ldots, M-1, \tag{5}$$

$$\boldsymbol{y}_{min} - \boldsymbol{s} \leq \boldsymbol{y}_j \leq \boldsymbol{y}_{max} + \boldsymbol{s}; \quad j = 1, 2, \ldots, N. \tag{6}$$

The comminution process used in this paper is illustrated in Figure 2. This plant consists of three areas. The first area is a material handling stockpile bunker with associated vibratory feeders. The second area is a closed comminution and sizing circuit. The final area is a material handling bin with three bin sections.

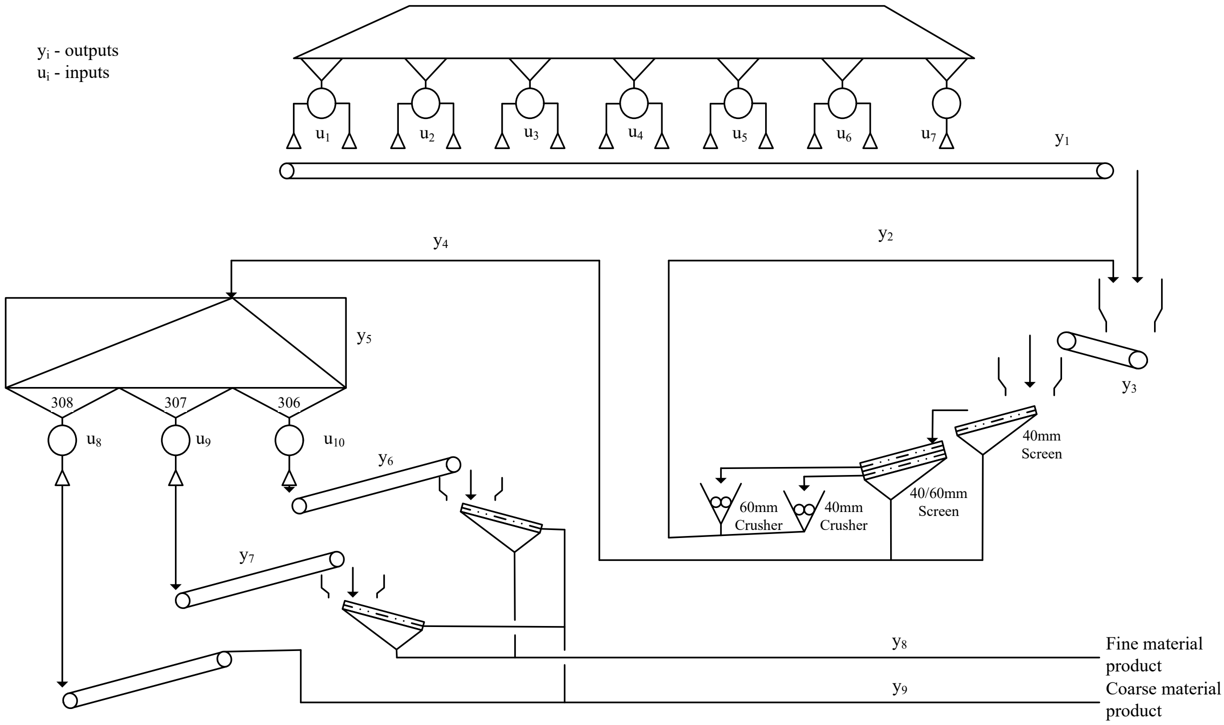

Figure 2: Process flow diagram showing the area affected by APC project.

The input process variables are:

- Coal stockpile feeder variable speed drive (VSD) speeds (u_1-u_7)
- Bin module 306, 307 and 308 feeder speeds (u_8-u_{10})

The output process variables are:

- Stockpile feed rate (y_1): measured
- Crushing and screening recycle flow rate (y_2): not-measured
- Primary screen feed mass flow rate (y_3): measured
- Bin feed rate (y_4): not measured
- Bin level (y_5): measured
- Bin module 306 and 307 discharge flow rates (y_6 and y_7): measured
- Fine material product flow rate (y_8): not-measured
- Coarse material product flow (y_9): measured

The stockpile bunker is fed by a primary crushing plant which sizes coal ROM to +40mm. Material is drawn from the bunker from seven different points through vibratory feeders. The ROM material from the bunker is comminuted and screened in closed circuit. The oversize stream is crushed with an 80mm sized double roll crusher while the undersize is crushed with a 40mm double roll crusher. The -40mm undersize mass flow is fed to a bin which acts as a buffer between the comminution and downstream coal separation plants. The bin area consists of three sections and is fed near the centre of the bin compartments. The bin sections are emptied using vibratory feeders while bin level is monitored.

The dynamic models developed for the different equipment in the comminution circuit are detailed in Meyer (2016). The bin model was developed in Meyer et al. (2015). These dynamic models act as the basis for the nonlinear MPC simulation described.

The system identification approach from Ljung (1987) is used for each model fit. Input-output data taken from an actual coal beneficiation plant production historian were used to fit the models. Two thirds of the production data were used to identify the models to allow for an additional one third of production data to be used for model validation.

The objectives (Steyn, 2014) of the NMPC for the circuit shown in Figure 2 were determined as follows:

- Primarily ensure that the bin never runs empty or overflows;
- Maximise plant throughput; and
- Ensure product bin mass flow rate is maintained in proportion with each other.

The simulations below illustrate the control of the feed bin and tests how the bin level can be used to change the NMPC objective function to focus on either throughput or maintain the bin level. The stockpile and comminution circuit can also be controlled, but are not shown in this paper. Further details on the control of these other areas are given in Meyer (2016).

For the feed bin area control simulation, it is assumed that the stockpile area is operated manually while the feed bin and DMS screen feed are controlled automatically. This implies that the mass flow from the stockpile area (y_1) is a measured disturbance (since it is the result of manually operating the seven stockpile feeder bunker areas). The screen and crushing process therefore simulates the resulting crusher recycle mass flow (y_2) and screen undersize mass flow (y_4) fed to the bin.

A comparison of the NMPC performance to the manually controlled situation is therefore possible since it is assumed the stockpile area is controlled manually. Production data that was used for the identification of the screen, crush and bin area models, are used to illustrate the feed bin controller. The manually operated plant response is compared to that of the simulated NMPC to illustrate the possible improvement in production throughput.

The feed bin area has competing objectives. The first objective is to maximise throughput to the dense medium separation (DMS) and cyclone (DMC) plants downstream while ensuring consistent control of the mass flows. The second objective is to ensure that the bin level does not run empty or overflow. By trying to maximise throughput, the bin will naturally run empty. If the feed to the bin becomes too high, the bin could overflow.

Figure 3 illustrates the varying objective of the bin system. At low and high bin levels (l_b < BL or l_b > BH) the objective of the controller should be to ensure the bin level reaches a point within safe limits (i.e. between BL and BH). This is to ensure the bin doesn't overflow or run empty. While the bin level is within safe limits (BL $\leq l_b \leq$ BH) the objective of the controller should be to maximise throughput. Maximising throughput is achieved by controlling module one and two undersize mass flow rates, and DMS plant one feed mass flow rates at desired reference trajectories.

Table 1 describes the associated codes and values that are used for the bin low and high levels.

Table 1: Bin NMPC objective function setup.

Code	Value	Units
BLL	15	%
BL	25	%
BH	75	%
BHH	85	%

The bin level (y_5) and DMS plant feed mass flow rates ($y_8\frac{y_6}{y_6+y_7}$, $y_8\frac{y_7}{y_6+y_7}$ and y_9) are controlled according to the objectives of the feed bin operation described above and the definition of the MPC objective function (Equation 3) with typical constraints (Equations 4, 5 and 6).

This means that the bin objective function for the NMPC is,

$$\boldsymbol{J}_{\text{bin}} = \sum_{j=1}^{N} ||\boldsymbol{\Gamma}_{\text{s,bin}}\mathbf{I}_4(\hat{\boldsymbol{y}}_{\text{bin},j} - \boldsymbol{y}_{s,\text{bin},j})||^2_{\mathbf{R}_{\text{bin}}} + \sum_{j=0}^{M-1} ||\Delta\boldsymbol{u}_{\text{bin},j}||^2_{\mathbf{P}_{\text{bin}}}, \tag{7}$$

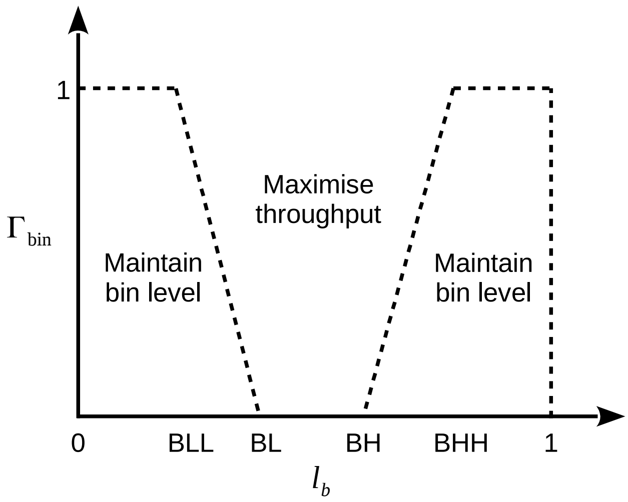

Figure 3: Feed bin control objective (Γ_{bin} = Objective function factor used in Equation 8; l_b = y_5).

where,

$$\boldsymbol{\Gamma}_{\text{s,bin}} = \begin{pmatrix} \Gamma_{\text{bin}} \\ 1 - \Gamma_{\text{bin}} \\ 1 - \Gamma_{\text{bin}} \\ 1 \end{pmatrix}, \tag{8}$$

the control horizon is two seconds (M = 2) and the prediction horizon is five seconds (N = 5). The bin objective is to ensure the bin level tracks a reference trajectory of 50% during high and low bin level limits (while Γ_{bin} = 1). During safe level limits (while Γ_{bin} = 0) objective function $\boldsymbol{J}_{\text{bin}}$ focuses on maintaining the throughput reference trajectories.

A weighting matrix of $\mathbf{R}_{\text{bin}} = 1000\mathbf{I}_4$ for the output error ($\hat{\boldsymbol{y}}_j - \boldsymbol{y}_s$) was used in the MPC objective function $\boldsymbol{J}_{bin}$. The output predictions for the bin ($\hat{\boldsymbol{y}}_{\text{bin},j}$) were defined as,

$$\hat{\boldsymbol{y}}_{\text{bin},j} = \begin{pmatrix} y_5 \\ y_8 \\ y_9 \\ y_8 \frac{y_6}{y_6 + y_7} \end{pmatrix}, \tag{9}$$

while the reference trajectory ($\boldsymbol{y}_{s,\text{bin},j}$) was selected as,

$$\boldsymbol{y}_{s,\text{bin}} = \begin{pmatrix} 50\% \\ 200\text{t/h} \\ 300\text{t/h} \\ y_8 \frac{y_7}{y_6 + y_7} \end{pmatrix}. \tag{10}$$

A weighting matrix of $\mathbf{P}_{\text{bin}} = 1000\mathbf{I}_2$ for the input changes ($\Delta\boldsymbol{u}_{\text{bin},j}$) was used while the inputs ($\boldsymbol{u}_{\text{bin},j}$) were defines as,

$$\boldsymbol{u}_{\text{bin},j} = \begin{pmatrix} u_9 \\ u_{10} \end{pmatrix}. \tag{11}$$

The input ($\boldsymbol{u}_{\text{bin},j}$) constraints of the bin are,

$$\mathbf{0} \leq \boldsymbol{u}_{\text{bin},j} \leq \mathbf{50}\text{t/h}, \tag{12}$$

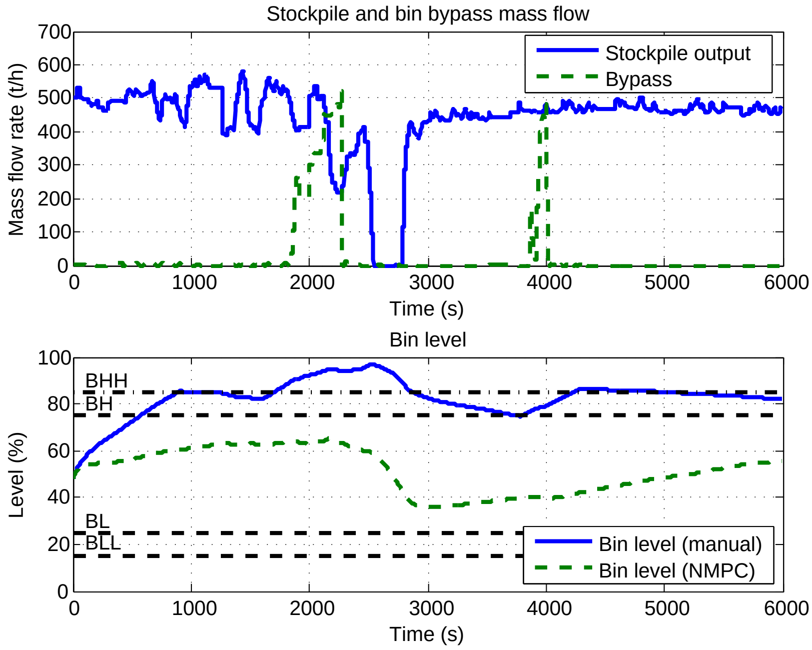

Figure 4: Bin NMPC measured disturbances with measured (manual) and simulated level comparison (Stockpile output = y_1; Bypass = u_8; Bin level = y_5).

and the predicted output ($\hat{\mathbf{y}}_{\text{bin},j}$) constraints are,

$$\begin{aligned} 0 &\leq \hat{y}_{\text{bin},1,j} \leq 100\%, \\ 0 &\leq \hat{y}_{\text{bin},2,j} \leq 350\text{t/h}, \\ 0 &\leq \hat{y}_{\text{bin},3,j} \leq 200\text{t/h}, \\ 0 &\leq \hat{y}_{\text{bin},4,j} \leq 200\text{t/h}. \end{aligned} \tag{13}$$

such that the inputs for the variable speed drive frequencies of all the feeders fall within operating ranges of 0Hz and 50Hz and the bin level remains within 0% and 100%. The DMS plant feed mass flow rates ($y_8\frac{y_6}{y_6+y_7}$, $y_8\frac{y_7}{y_6+y_7}$ and y_9) are also constrained within acceptable limits (Module one and two mass flow rates fall within 0 and 200t/h while the mass flow rate DMS plant number 1 is within 0 and 350 t/h).

With the objective function and constraints defined, the process is simulated using NMPC. The nonlinear dynamic bin model is used for the NMPC future prediction and the control simulation of the bin and DMS plant feeds. The NMPC problem can be solved by using the nonlinear programming problem. The objective function (7) is minimised over control moves subject to plant dynamics and input/output constraints detailed above.

Each NMPC simulation input and output are shown in comparison to the actual plant values during manual operation. Figure 4 shows actual measured disturbances (stockpile and bin bypass) used to simulate the stockpile feed to the process. Figure 4 also shows the bin level response with associated objective limits (BLL, BL, BH BHH) as described in Figure 3.

Figure 5 illustrates the NMPC control moves compared to the actual plant inputs. These outputs are compared to that of the actual plant output where manual control was applied. Figures 6 and 7 show the final control objectives where the feeds to the DMS plants ($y_8\frac{y_6}{y_6+y_7}$, $y_8\frac{y_7}{y_6+y_7}$ and y_9) are maximised by controlling them at desired reference trajectories. The desired reference trajectories are the same as the manual control of the plant.

In order to measure the performance of the NMPC when compared to that of the actual plant output, a comparison between the manually operated bin throughput and NMPC throughput per DMS plant feed and total throughput are determined. The percentages of gains or losses in throughput are also determined. Gains are represented as positive numbers while losses are represented as negative numbers. Table 2 shows a summary of the NMPC performance

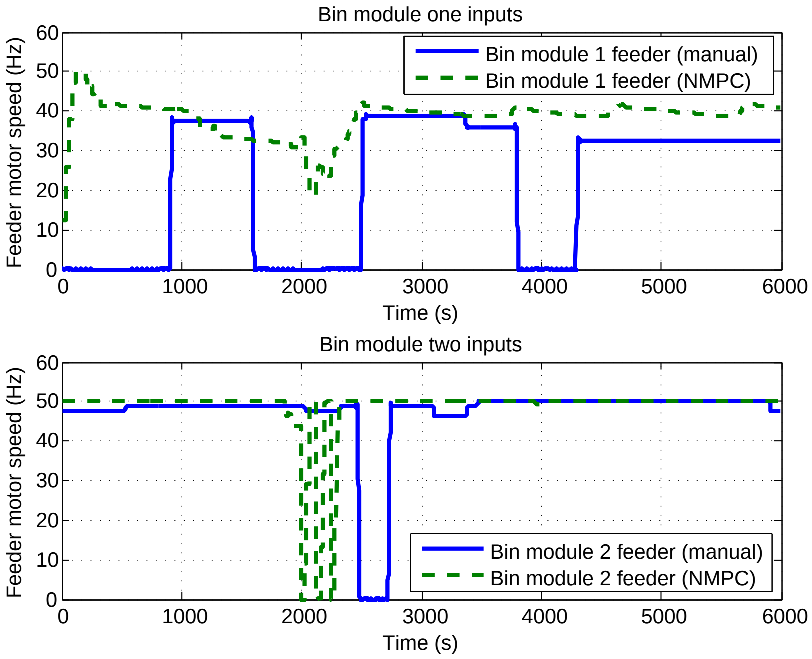

Figure 5: Bin NMPC measured (manual) and simulated motor feeder manipulated variable comparison (Bin module 1 feeder = u_9; Bin module 2 feeder = u_{10}).

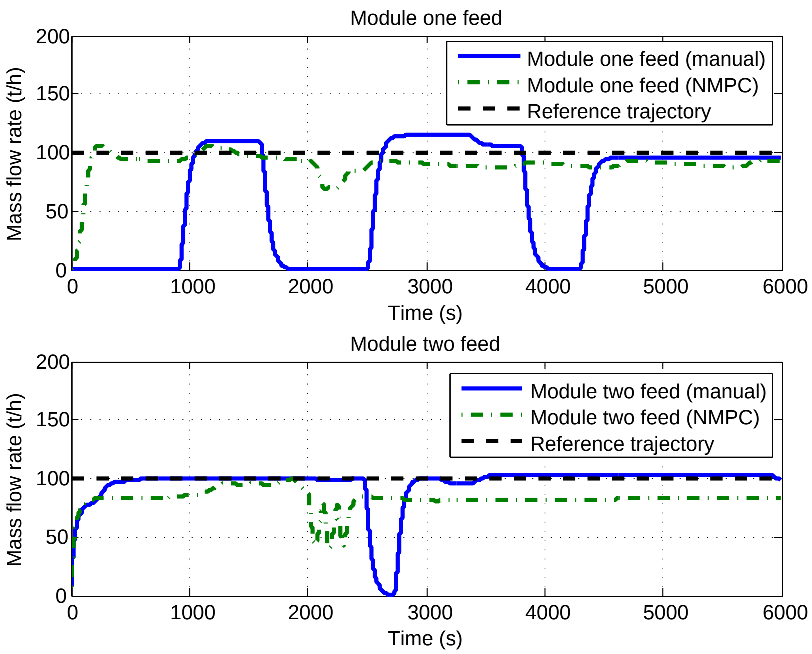

Figure 6: Bin NMPC measured (manual) and simulated module one and two feed comparison (Module one feed = $y_8 \frac{y_6}{y_6+y_7}$; Module two feed = $y_8 \frac{y_7}{y_6+y_7}$).

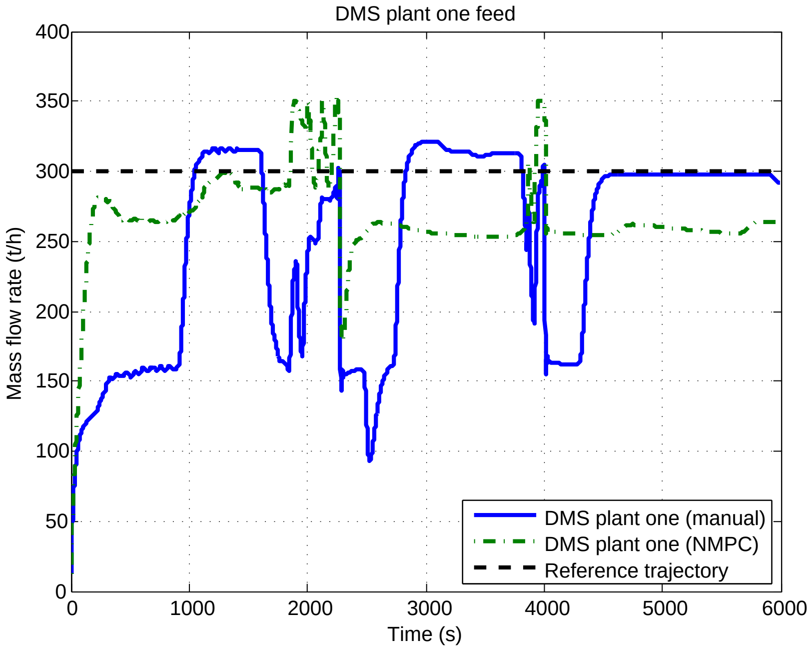

Figure 7: Bin NMPC measured (manual) and simulated DMS plant one feed comparison (DMS plant one feed = y_9).

Table 2: Bin manual control versus NMPC performance evaluation (Gains are represented as positive numbers while losses are represented as negative numbers).

Performance area/measure	Manual control (t)	NMPC (t)	Gain/loss (%)
Module one feed	105	150	43.5
Module two feed	159	138	-13.5
DMS plant one feed	412	443	7.5
Total	676	700	3.6

versus the actual feed bin operation with manual control.

Figure 4 illustrates the measured disturbance from the stockpile area and the associated bin level response based on the NMPC control moves. The benefit of having the input as a measured disturbance in this simulation is that it is possible to compare the NMPC performance to that of the manually operated plant. The controller keeps the bin level within the specified level limits for maximum throughput.

Figure 6 illustrates how the NMPC was able to ensure the feed to the two DMC modules was kept in balance while maintaining a reference trajectory of 100 t/h. Similarly, Figure 7 shows how the feed to the DMS plant one tries to maintain a rate of 300 t/h. The simulation also incorporates another measured disturbance which is the bin bypass mass flow rate. This bypass is manually actuated by a flap gate. It can be seen that during the time intervals the bypass was opened (Figure 4), around 2000 seconds and again around 4000 seconds, the feed to DMS plant one increased significantly. This is because the bypass essentially goes toward the DMS plant one in the case when the bin modules one and two mass flow rates are starved. The upper constraint of 350 t/h in the DMS plant feed mass flow rate causes the NMPC to react by switching off the bin feeder module two as shown in Figure 5.

When comparing the NMPC performance to the manual operation, there was an overall improvement in throughput of 3.6%. Another important benefit is that the bin level was controlled within safe limits whereas the manually operated plant was dangerously close to having the bin overflow. Since the simulated increase in throughput was performed over a relatively short time frame, the potential improvement was projected over a much longer time frame of about 3 months using historical production data. During this evaluation, it was projected that by applying MPC to this particular coal comminution circuit would allow a potential increase in throughput of up to 5%. Other benefits of improved ROM bunker control and a more steady feed to downstream separation circuits were also factored into this performance improvement estimate.

A business case developed based on a 5% increase in throughput and prevailing coal prices, projected that the implementation of MPC would yield a net present value of ZAR 79 million, an internal rate of return of 380% and payback period of four months.

3. Implementation

The potential process improvement and business case from the NMPC simulation in Section 2 initiated a project at Exxaro Resources Grootegeluk Mine, Limpopo, South Africa. After a tender process, GE were awarded a contract to implement their APC solution on the Grootegeluk 5 (GG5) plant. The GE Digital Mine CSense MPC technology was used for the implementation and is described in more detail in this section.

In reference to the actual process flow diagram depicted in Figure 2, the control system objective for GG5 plant is to maintain maximum allowed throughput (y_1) to the crusher and screening circuit without violating the upper constraints on the recycle load (y_2) and primary screen (40mm) feed (y_3). The bin level (y_5), can surge between specified limits but the bin module 306 (y_6) and 307 (y_7) screen feed, as well as fine material (y_8) and coarse material (y_9) product flow, should not exceed plant upper constraints. The control system writes out to the stockpile feeder variable speed drives (u_1-u_7) to maintain throughput, as well as to the bin feeder variable speed drives (u_9-u_{10}) to regulate the level within surge limits, while taking all the above-mentioned constraints into consideration.

3.1. GE CSense MPC description

The CSense MPC (General Electric, 2016) is a real-time, industrial model predictive controller and system identification tool that extracts dynamic transfer function models from closed or open loop process data. These dynamic models are then used in the quadratic programming algorithm of the MPC to calculate the optimal control steps for the process that is to be controlled. The features include:

- Quadratic programming (QP) to solve for future control moves by minimising the controller objective function;
- Weighting matrices to give relative importance in the controller objective function to manipulated variable (MV) movements and control variable (CV) actions;
- Constraint specification to specify MVs and MV move rates as well as double upper and lower limits on CVs for better range control;
- Enabling and disabling of MVs, CVs and disturbance variables (DVs);
- System identification routines that can extract transfer function coefficients from historical data; and
- Web access for remote monitoring and tuning of the MPC controller.

3.1.1. System Identification

System identification refers to the procedure to extract dynamic process models from historical plant data (Ljung, 1987). Key to obtaining reliable dynamic models of the process is the quality of plant data with sufficient excitation in the MVs. The most ideal dataset for system identification are generated through a planned step test campaign where the MVs of the process are individually kept constant in an open loop environment and then stepped. Resulting CV responses are then due to a single, known MV action. Both model type and parameters can be extracted with high confidence in model accuracy from such datasets. Getting or generating step test data like this is not always easy or even possible. In such cases the data available must suffice with the knowledge that model mismatch could be present that will degrade MPC controller performance (see e.g. Olivier and Craig, 2013).

There are many techniques to perform system identification. The CSense MPC makes use of a time domain based technique that uses non-linear optimisation to fit model parameters to experimental data. The non-linear optimisation algorithm being used is Differential Evolution (DE) (Yao and Ge, 2018). The DE algorithm minimizes the sum of squared errors between the actual data and the outputs of a selected model. DE works by having a population of candidate solutions that are moved around in the search-space by using simple mathematical formula to combine the positions of existing agents from the population. If the new position of an agent is an improvement it is accepted and forms part of the population, otherwise the new position is simply discarded. The process is repeated and by doing so a satisfactory solution will eventually be discovered.

A detailed nonlinear model of the feed bin as shown in Figure 2 is given in Meyer et al. (2015). This model was used in a nonlinear MPC simulation, described in Section 2, in order to justify the funding required for an industrial implementation of MPC control. An advanced control technique such as MPC is model based and requires a plant model to function. Planned step tests were therefore performed on the GG5 plant. It was found that the plant responses of the coal comminution circuit are approximately linear in the region of operation, even though the feed bin model is not, and the step responses where thus used to determine the linear Laplace transfer functions shown in Table 3. These step responses where used to identify unknown linear Laplace transfer function parameters. Two plant models were developed with the first model (CV-MV 8x9 model matrix) representing eight CVs (y_1, y_3 and y_{5-10}) and nine MVs (u_{1-7} and u_{9-10}). The second plant model (CV-DV 8x1 model matrix) represents the eight CVs and one DV (u_8). The resulting Laplace transfer functions are given in Tables 3 and 4.

Table 3: Linear transfer functions for CV-MV 8x9 model matrix.

	u_1	u_2	u_3	u_4	u_5	u_6	u_7	u_9	u_{10}
y_1	$\frac{8e^{-20s}}{40s+1}$	$\frac{4.8e^{-17s}}{35s+1}$	$\frac{4.8e^{-15s}}{35s+1}$	$\frac{5.3e^{-10s}}{40s+1}$	$\frac{8e^{-5s}}{34s+1}$	$\frac{4e^{-10s}}{28s+1}$	$\frac{5}{32s+1}$		
y_3	$\frac{8e^{-20s}}{40s+1}$	$\frac{4.8e^{-17s}}{35s+1}$	$\frac{4.8e^{-15s}}{35s+1}$	$\frac{5.3e^{-10s}}{40s+1}$	$\frac{8e^{-5s}}{34s+1}$	$\frac{4e^{-10s}}{28s+1}$	$\frac{5}{32s+1}$		
y_5	$\frac{0.0016e^{-20s}}{s(40s+1)}$	$\frac{0.00096e^{-17s}}{s(35s+1)}$	$\frac{0.00096e^{-15s}}{s(35s+1)}$	$\frac{0.00106e^{-10s}}{s(40s+1)}$	$\frac{0.0016e^{-5s}}{s(34s+1)}$	$\frac{0.0008e^{-10s}}{s(28s+1)}$	$\frac{0.001}{s(32s+1)}$	$\frac{-0.0014}{s(27s+1)}$	$\frac{-0.0014}{s(27s+1)}$
y_6									$\frac{7}{27s+1}$
y_7								$\frac{7}{27s+1}$	
y_8								$\frac{4.2}{42s+1}$	$\frac{4.2}{42s+1}$
y_9									$\frac{2.8}{42s+1}$
y_{10}								$\frac{2.8}{42s+1}$	

Table 4: Linear transfer functions for CV-DV 8x1 model matrix.

	u_8
y_1	
y_3	
y_5	$\frac{-0.0002}{s}$
y_6	
y_7	
y_8	$\frac{1}{30s+1}$
y_9	
y_{10}	

3.2. MPC configuration

The QP objective function which is used accommodates set-point tracking, move suppression and soft constraint weighting is given below,

$$\boldsymbol{J}_{\text{MPC}} = \sum_{j=1}^{N} ||\boldsymbol{y}_j - \boldsymbol{r}||^2_{\boldsymbol{\Gamma}^y} + \sum_{j=1}^{M} ||\Delta \boldsymbol{u}_j||^2_{\boldsymbol{\Gamma}^u} + \sum_{j=1}^{N} ||\boldsymbol{\epsilon}^2_{\rho}||, \tag{14}$$

where $\Delta \boldsymbol{u}$ represents the change in manipulated inputs (controller moves) from one sampling instant to the next, $\boldsymbol{y}$ the outputs from the process, $\boldsymbol{r}$ the reference signal and $\boldsymbol{\epsilon}$ the amount by which an output violates a constraint. $\boldsymbol{\Gamma}^y$ is a diagonal weighting matrix determining the importance of the reference tracking of each output. $\boldsymbol{\Gamma}^u$ is a diagonal weighting matrix for the move suppression and $\boldsymbol{\rho}$ is a weighting factor for each constraint violation. The situation is illustrated in the figure below and associated variables are describes in Table 5.

Table 5: Definition of variables used in QP objective function with set-point tracking.

Variable	Definition
N	Prediction horizon
M	Control horizon
rateUp.U	Maximum positive rate of change for input $\boldsymbol{u}$
-rateDown.U	Maximum negative rate of change for input $\boldsymbol{u}$
high.U	Upper limit for input $\boldsymbol{u}$
low.U	Lower limit for input $\boldsymbol{u}$
ucurrent	Latest/newest calculated value for input $\boldsymbol{u}$
sh1	Soft upper constraint - high limit (soft upper constraint weight applicable when output $\boldsymbol{y}$ projection at each discrete interval violates this limit)
sh2	Soft upper constraint - high high limit (soft upper constraint weight amplified ten times when output $\boldsymbol{y}$ projection at each discrete interval violates this limit)
sl1	Soft lower constraint - low limit (soft lower constraint weight applicable when output $\boldsymbol{y}$ projection at each discrete interval violates this limit)
sl2	Soft lower constraint - low low limit (soft lower constraint weight amplified ten times when output $\boldsymbol{y}$ projection at each discrete interval violates this limit)
εu1	Amount by which output $\boldsymbol{y}$ violates sh1
εu2	Amount by which output $\boldsymbol{y}$ violates sh2
εl1	Amount by which output $\boldsymbol{y}$ violates sl1
εl2	Amount by which output $\boldsymbol{y}$ violates sl2

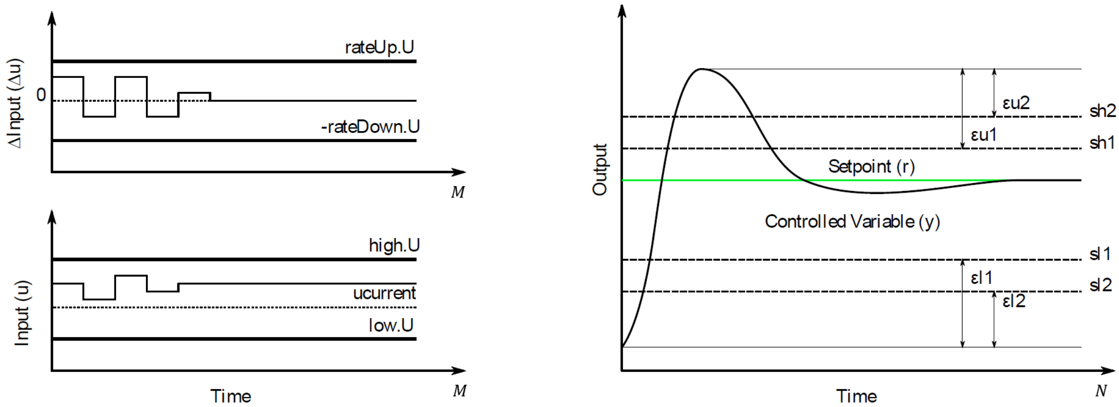

Figure 8: Illustration of QP objective function accommodating set-point tracking.

The optimization problem is quadratic in nature and this makes it possible to apply well-known QP solvers (see e.g. Boyd et al., 1998; Bartlett et al., 2002). It was found that the interior point algorithm is most suited to the overall MPC problem and can solve large scale problems in a relatively small duration. The key variables used within the QP and their affect are listed below:

- *Inputs to the QP algorithm:*
  - **Maximum iterations:** The maximum number of iterations used to solve the problem can be specified. If this number is surpassed the algorithm will stop and return the current value.
  - **Tolerance:** After each iteration a complimentary gap (minimum allowed difference in error for the optimizer between iterations where it will stop even if it did not converge to the optimal solution) is calculated and a tolerance on this value must be specified. Once the tolerance is achieved the output flag will be set to one indicating that a feasible solution has been found and the algorithm will then terminate.

- **Starting point:** The algorithm must be given a starting point initial state and for the MPC problem the previous solution is used.

- *Outputs of the QP algorithm:*
  - **Feasibility flag:** If a solution satisfying a predefined tolerance on the complimentary gap has been found the feasibility flag will be set to 1.
  - **Objective function value:** The minimum value of the objective function found by the algorithm.
  - **Iterations:** The total number of iterations used within the algorithm is returned.
  - **Solution time:** The time taken by the solver to find a solution.

The objective function contains the weighting matrices for the MVs, the CVs and the constraints. Constraints on the MVs, MV move rates, the soft and hard limits of the CVs can also be obtained in the objective function. The slack variable is considered as the soft constraint. Tables 6, 7, 8 and 9 show the software configuration of the objective function for the GG5 plant CSense MPC implementation.

Table 6: CSense MPC software parameter configuration.

Parameter	Value
Sample interval	4
Prediction horizon (N)	20
Control horizon (M)	10

Table 7: CSense MPC software CV configuration.

Variable	Lower range	Upper range	Hard lower constraint	Soft lower constraint	Soft upper constraint	Hard upper constraint	Weight	Constraint softening lower weight	Constraint softening upper weight	Integrating	Filter time constant
y_1	0	700	0	0	700	700	1	0	2	No	0.5
y_3	0	1000	0	0	900	1000	0	0	2	No	0.5
y_5	0	100	0	20	80	100	1	0	2	Yes	0.5
y_6	0	100	0	0	400	500	0	0	2	No	0.5
y_7	0	100	0	0	400	500	0	0	2	No	0.5
y_8	0	500	0	0	400	500	0	0	2	No	0.5
y_9	0	300	0	0	200	500	0	0	2	No	0.5
y_{10}	0	300	0	0	200	500	0	0	2	No	0.5

Table 8: CSense MPC software MV configuration.

Variable	Lower range	Upper range	Lower constraint	Upper constraint	Max negative constraint	Max positive constraint	Weight
u_1	50	100	50	100	-10	10	1
u_2	50	100	50	100	-10	10	1
u_3	50	100	50	100	-10	10	1
u_4	50	100	50	100	-10	10	1
u_5	50	100	50	100	-10	10	1
u_6	50	100	50	100	-10	10	1
u_7	50	100	50	100	-10	10	1
u_9	50	100	50	100	-10	10	0.2
u_{10}	50	100	50	100	-10	10	0.2

Table 9: CSense MPC software DV configuration.

Variable	Lower range	Upper range
u_8	0	100

3.3. CSense MPC on/off test results

After the CSense MPC software was installed on the GG5 plant automation system, it was configured with the above explained linear transfer function matrix models and objective function configuration. The CSense MPC was tested over one day of operation on the actual plant through a series of on/off tests. While the MPC was turned off, the operator was responsible for activating or deactivating the MVs.

The figures below show the results of the on/off tests performed using the CSense MPC reporting system. Figure 9 illustrates the on/off testing of the MPC and plant MVs (u_{1-7}). Figure 10 shows the response of the bin level (y_5) during the on/off testing of the MPC. Figure 11 and Figure 12 illustrate the throughput response (y_6 and y_7) of the MPC during the on/off testing. These results indicate that the CSense MPC can control bin level and throughput according to the objective function configuration described in Section 3.2. The operator can change the MPC setpoints and constraints during operation. Such changes are visible in Figure 10 where the bin level setpoint and maximum contraint were changed. A long term analysis of the MPC controller in done in Section 4.

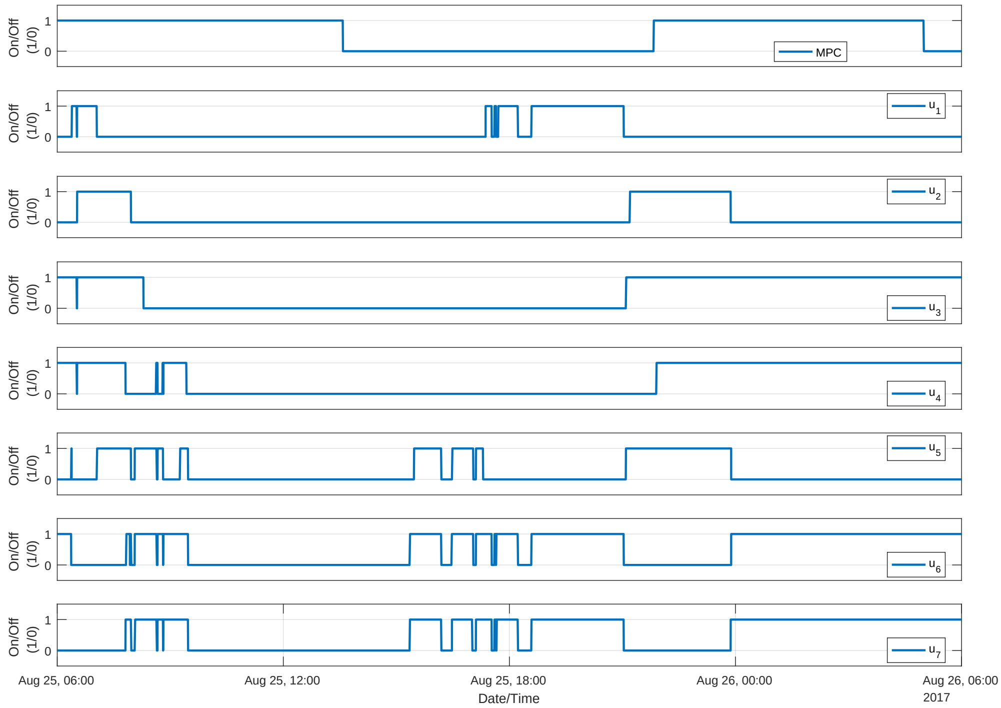

Figure 9: GG5 plant CSense MPC on/off tests illustrating MVs (u_{1-7}).

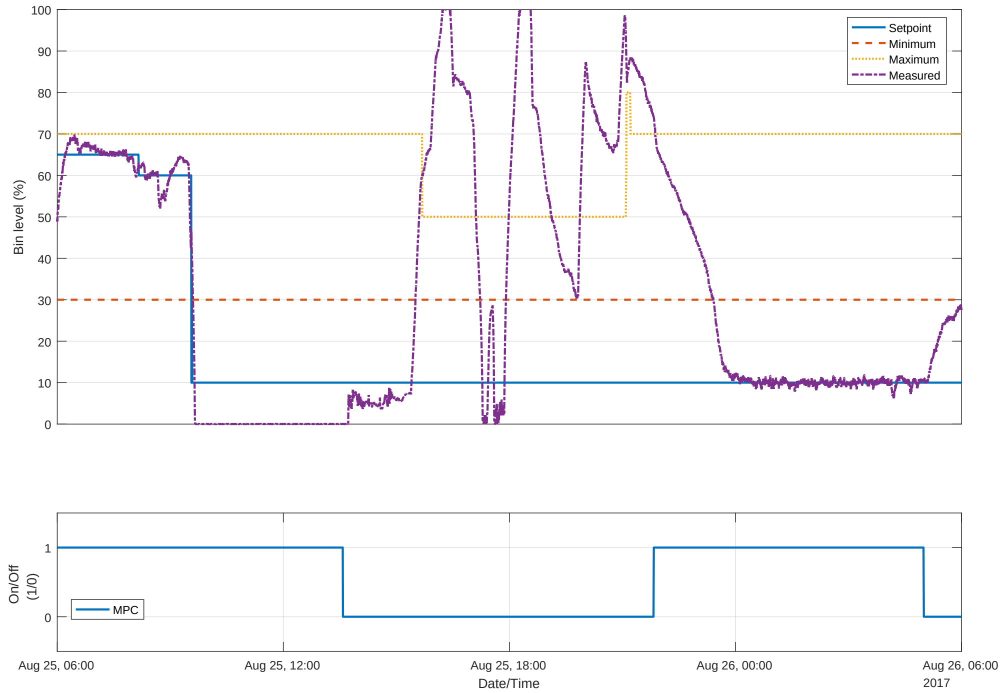

Figure 10: GG5 plant CSense MPC on/off tests illustrating bin level (y_5).

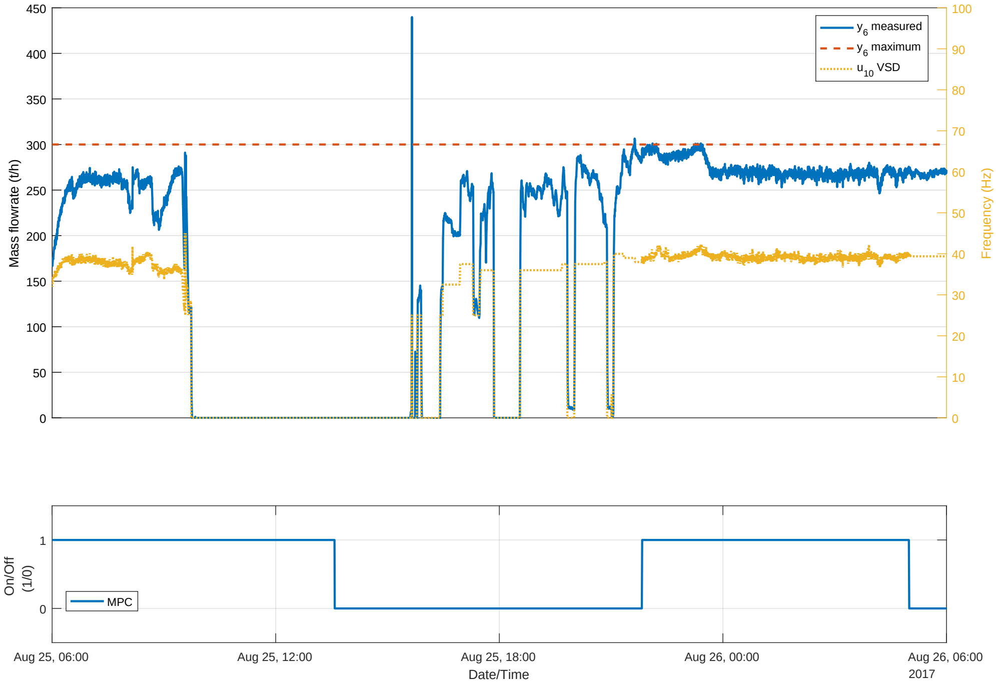

Figure 11: GG5 plant CSense MPC on/off tests illustrating y_6 feeder response.

Figure 12: GG5 plant CSense MPC on/off tests illustrating y_7 feeder response.

3.4. Solution monitoring and maintenance

A key metric highlighting the success of the solution is the APC utilization. The operator is ultimately the end user: when the end user notices that the solution is not able to achieve expected results or reject unexpected disturbances, they have full control to deactivate the controller thereby decreasing APC utilization. This metric was maximised by continuous remote monitoring, maintenance and people engagement, especially during the commissioning phase.

An APC solution such as MPC requires attention to maintain its effectiveness (Ford, 2009). For example, a process change might fall outside of the nominal operating regime of the solution and therefore require maintenance. A method for addressing this problem is to continuously monitor and capture data related to the performance of the APC. This allows staff at various organisational levels to monitor and participate in ensuring that goals of the APC are met. In particular, such monitoring enables the solution engineer to investigate reasons for the underutilization of the APC. Site operators and engineers can then be engaged to help in the development and implementation of features aimed at avoiding future underutilization. Furthermore, the engagement allows for more effective change management and contributes to the development of an understanding of the process, particularly during commissioning and early after the go-live milestone.

The average utilization time after commissioning was approximately 11.4 months, illustrating the benefits of the GE Digital Mine solution to operations.

4. Performance assessment

The MPC implementation described in Section 3 is one of two APC strategies implemented by GE on the GG5 plant. The aim of this section is to perform an evaluation of the implemented APC strategies, in particular to evaluate if the envisaged 5% increase in throughput for the process was achieved. Initially an experimental design approach was proposed to evaluate the controller performance objectively (Craig and Koch, 2003; Bauer and Craig, 2008), but for various reasons such an approach was not employed. One reason is that such an approach would imply toggling between the old pre-APC system and the new APC system which is difficult to motivate when the new controller is seen to perform substantially better.

GE implemented two APC strategies – an ARC was implemented on 13 August 2017 and a linear MPC was implemented on 24 October 2017. Data sampled at one second intervals for the period 1 June 2017 to 24 December 2017 were evaluated and separated in two sections – a pre-APC section from 1 June 2017 to 9 August 2017 (5,750,201 useable data points), and an APC section from 15 August 2017 to 24 December 2017 (6,767,808 useable data points). Some sections in these date ranges were left out due to incidents of spontaneous combustion or white stones at the relevant stockpiles (as noted by Grootegeluk staff), and due to data errors (values approaching infinity).

No attempt was made to exclude data when the plant was not operating normally, e.g. when maintenance was done. Given the number of data points used and the method of data analysis, it is not unreasonable to assume that both the pre-APC and APC periods are effected by such events equally.

4.1. Data analysis

The data analysis focused on two variables in particular: the main plant feed rate (y_1 in Figure 2); and the bin level (y_5 in Figure 2).

Figure 13 shows a histogram of the “raw” one-second interval bin level data for both the pre-APC and APC periods. The bin level is included here as the controller implementation described in this paper has its roots in an investigation aimed at improving bin level control (Meyer, 2016).

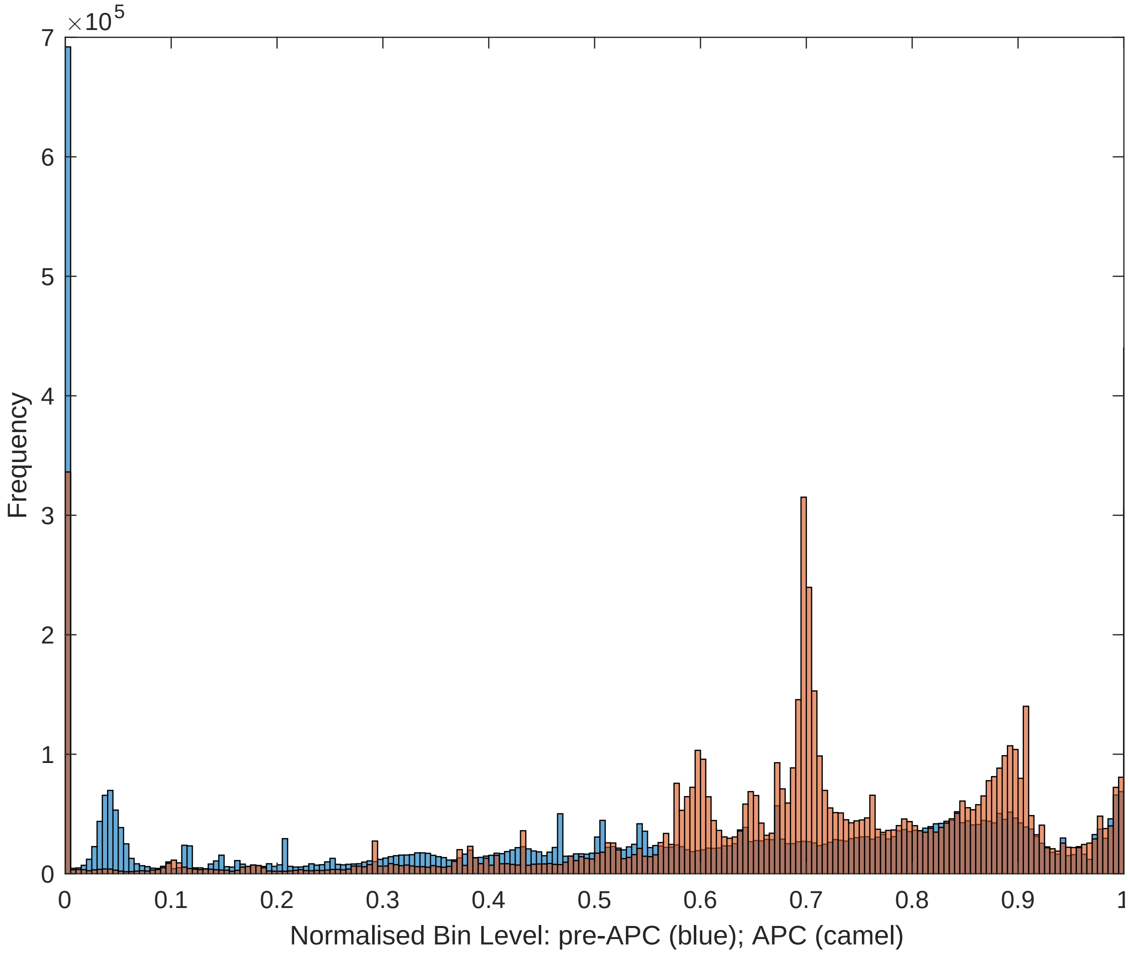

Figure 13: Histograms of normalised bin level: pre-APC from 1 June 2017 to 9 August 2017 (blue); APC from 15 August 2017 to 24 December 2017 (camel).

Some form of bin level control is evident from the APC bin level histograms in Figure 13. During the approximately four months of APC operation, the bin level setpoint was mostly set at 0.6, 0.7 and 0.9, hence the clustering around these values in Figure 13. No automatic bin level control was used during the pre-APC period (blue bars in Figure 13), resulting in numerous plant stoppages. As shown in Table 10, this fact is apparent from the reduced standard deviation of the bin level for the APC period. (The bin level is 0 or 1 when the plant is not operating).

Table 10: Means, medians and standard deviations of useable "raw" one-second interval data.

Variable	**Median**	**Mean**	**Standard deviation**
Throughput pre-APC (t/h)	417.77	287.54	233.17
Throughput APC (t/h)	425.59	311.19	238.18
Normalised Bin Level pre-APC	0.6415	0.5631	0.3440
Normalised Bin Level APC	0.7060	0.6868	0.2451

Figure 14 shows the useable plant throughput data in histogram form as measured for both the pre-APC and APC periods.

The histogram bins below 150 t/h were excluded from Figure 14 for both periods in order to better visualize the impact of the APC. It would appear from Figure 14 that the APC does increase throughput. This fact is also borne out by the mean throughputs shown in Table 10. The observed difference in means is 311.9-287.54=23.65 t/h which is equivalent to an increase of about 8.22%. The question of whether this increase is statistically significant, is addressed next.

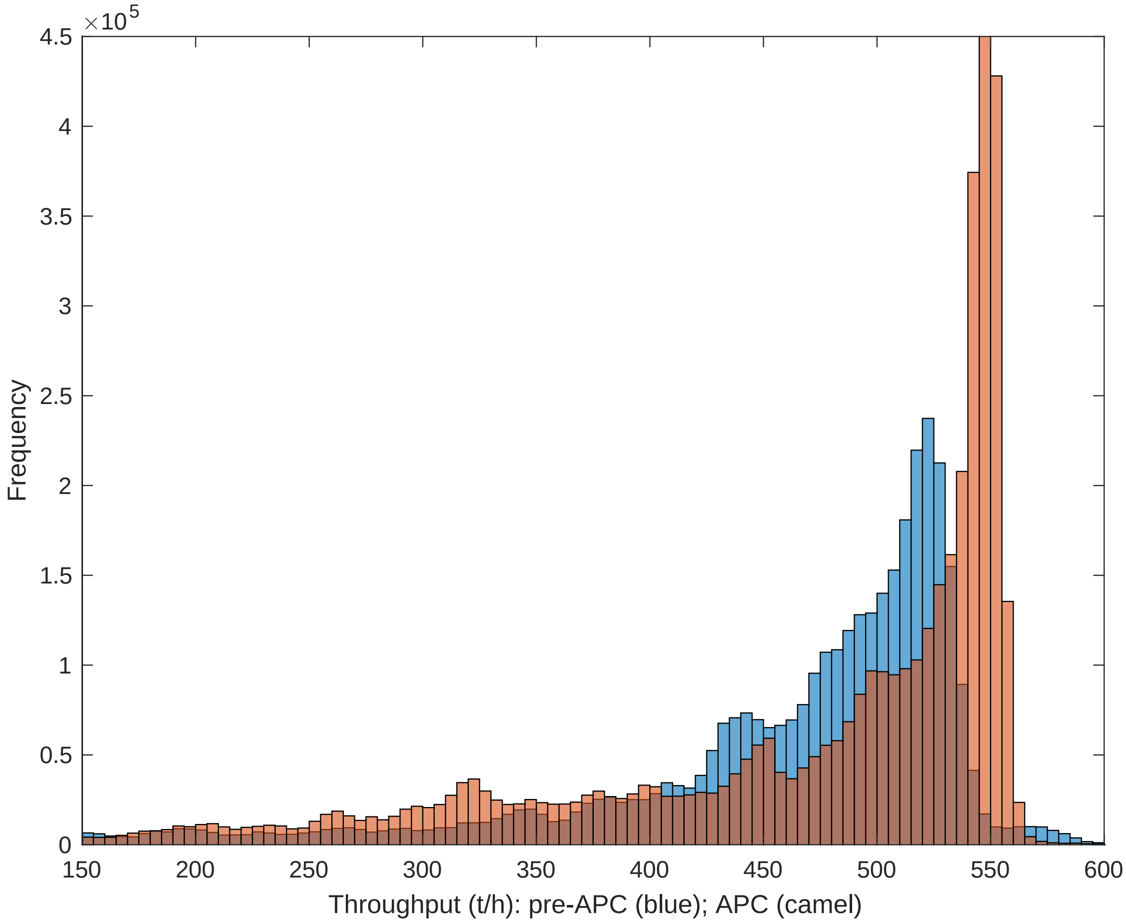

Figure 14: Histograms of throughput: pre-APC from 1 June 2017 to 9 August 2017 (blue); APC from 15 August 2017 to 24 December 2017 (camel).

4.2. *Statistical analysis*

Statistical analysis is done in this section in the form of a hypothesis test. Numerous tests are available for the testing of hypotheses. Which test to use depends on e.g. the assumptions under which the test is valid, the effect of violating these assumptions, and the type of errors associated with each test.

A Monte-Carlo permutation test, a Wilcoxon rank-sum test, and a two sample t-test were performed on the throughput data, all yielding similar results. In this section only the Monte-Carlo permutation test is described due to the relatively weak assumptions under which the test results are valid (see e.g. Good, 2005).

The hypothesis to be tested can be written as:

$$H_0 : \eta_A = \eta_B \tag{15}$$

$$H_1 : \eta_A < \eta_B \tag{16}$$

where η_A and η_B are the throughput population means and subscript A refers to the pre-APC throughput, and subscript B refers to the APC throughput. It is assumed under the null hypothesis H_0 that the throughput population means are equal. The alternate hypothesis H_1 states that the APC throughput is higher than the pre-APC throughput.

4.3. Monte-Carlo permutation test

Under the null hypothesis the two populations are equal and therefore it can be assumed that the pre-APC and APC labels may be interchanged. There are n_A = 5,750,201 and n_B = 6,767,808 observations in the pre-APC and APC populations respectively with a total of n_{tot} = 12,518,009 observations in the combined set. The combined set can be split into populations of sizes n_A and n_B in $\binom{n_{tot}}{n_B}$ different ways.

As it is infeasible to perform a permutation to determine the full distribution, a Monte-Carlo permutation test was performed to generate a 1000 samples of differences between means (Good, 2005). The 1000 samples were obtained by randomly selecting 1000 populations of sizes n_A and n_B, and calculating the differences between the sample means. The percentage change in the two populations is used as a test statistic, i.e. $(311.9/287.54 - 1) \times 100 = 8.22\%$.

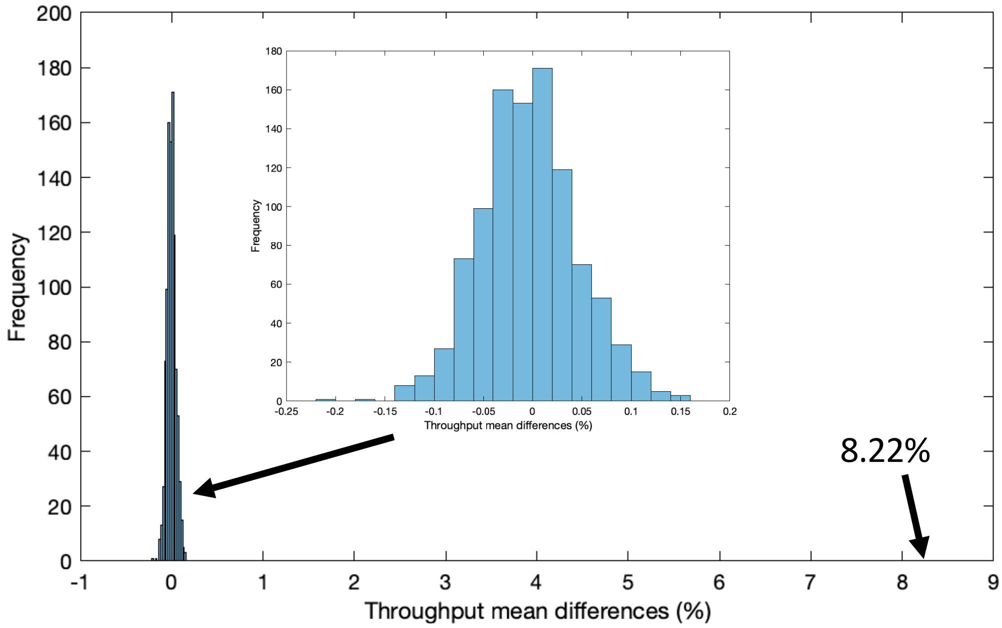

Figure 15: Histogram of the 1000 mean differences generated from a Monte-Carlo permutation test.

Figure 15 shows a histogram of a 1000 differences between sample means of size n_B and size n_A, as generated by the Monte-Carlo permutation test. This histogram represents the mean differences that can be expected to occur due to chance, with the maximum of the 1000 mean differences generated being 0.15%. A mean difference of 8.22% as found in the trial is therefore highly unlikely to occur by chance as it is more than an order of magnitude larger than 0.15%, and hence the difference of 8.22% is statistically significant. The alternate hypothesis is therefore valid, i.e. the implementation of APC led to an increase in throughput.

The significant 8.22% increase in throughput at 2018 coal prices during the implementation of the APC realised an actual net present value of ZAR 88.8 million, an internal rate of return of 725% and payback period of less than two months. All financial evaluations incorporate upstream and plant availability, cost of implementation and a 20 year lifecycle interval.

5. Conclusion

MPC can be implemented with very successful results in coal comminution by following a general control framework. A summary of the steps followed were:

- Obtain a mathematical model of a real plant;
- Design and simulate a controller using the mathematical model;

- Determine the potential economic performance and develop a business case from simulation;
- Implement a controller on a real plant; and
- Evaluate the economic performance of the implemented controller.

Initially the communition plant was modelled from a theoretical perspective using first principal nonlinear dynamic models. These models were identified with actual plant data to ensure the process is simulated with sufficient accuracy to be used for controller design. An appropriate objective function was designed to maximise throughput and to maintain bin level. This objective function was used to simulate NMPC using the plant model. After evaluating the NMPC simulation output and considering various other factors such as downstream improvement by having more stable operations and improved production availability, a 5% increase in throughput was estimated. This potential performance improvement was used to develop a business case to implement APC on the actual plant.

Exxaro selected GE through a tender process to implement the actual APC solution on the GG5 comminution circuit of the Grootegeluk coal mine. Both ARC and linear MPC were implemented. Details of the linear MPC implementation are described in Section 3 as it is more comparable to the simulated NMPC of Section 2.

A statistical performance assessment was conducted on production throughput using about 6 months of actual plant data. It was found that APC achieved an 8.22% increase in throughput.

Table 11 summarises the key performance metrics (production and financial) of the simulated and actual controller.

Table 11: Summary of production and economic performance improvement between the simulated and actual controller.

Key performance metric	Simulated controller	Actual controller
Throughput increase (%)	5	8.22
Net present value (ZAR million)	79	88.8
Internal rate of return (%)	380	725
Payback period (months)	4	1.7

Apart from the above mentioned production and economic performance improvements, the following secondary benefits were also realised:

- Stabilising the process from upstream disturbances (e.g. mining activities);
- Ensuring downstream processes (DMS and DMC plants) receive a constant and consistent supply of sized ROM;
- Increased process availability as bin level is maintained eliminating possible downstream supply issues;
- Eliminate the need for manual bypass operation in case of downstream supply shortages; and
- Allow operators to concentrate on other process or material related improvements.

With the success of this work, the possibility of implementing APC technologies at other Exxaro Grootegeluk coal plants and Exxaro coal business units should be explored. This also poses the question on how much improvement is possible in the mining industry in general through the use of APC.

6. Acknowledgement

This work is based on research supported in part by the National Research Foundation of South Africa (IRC grant number 111741). The authors gratefully acknowledge Grootegeluk Coal Mine and GE's Digital Mine for the use of the data shown in this paper.

References

Bartlett, R.A., Biegler, L.T., Backstrom, J., Gopal, V., 2002. Quadratic programming algorithms for large-scale model predictive control. Journal of Process Control 12, 775–795.

Bauer, M., Craig, I.K., 2008. Economic assessment of advanced process control - a survey and framework. Journal of Process Control 18, 2–18.

Boyd, S., Crusius, C., Hansson, A., 1998. Control applications of nonlinear convex programming. Journal of Process Control 8, 313–324.

Camacho, E., Bordons, C., 2004. Model predictive control. Advanced Textbooks in Control and Signal Processing. 2 ed., Springer-Verlag, London.

Cortinovis, A., Mercangoez, M., Mathur, T., Poland, J., Blaumann, M., 2013. Nonlinear coal mill modeling and its application to model predictive control. Control Engineering Practice 21, 308–320.

Craig, I., Koch, I., 2003. Experimental design for the economic performance evaluation of industrial controllers. Control Engineering Practice 11, 57–66.

Craig, I.K., Henning, R.G.D., 2000. Evaluation of advanced industrial control projects: a framework for determining economic benefits. Control Engineering Practice 8, 769–780.

Ford, J., 2009. APC - Productivity tool or shelfware? `https://www.controlglobal.com/articles/2009/APC0904/`. Accessed: 03-11-2018.

General Electric, 2016. CSense 6.0 from GE Digital. `https://www.ge.com/digital/sites/default/files/download_assets/csense-from-ge-digital-datasheet.pdf`. Accessed: 24-11-2018.

Good, P.I., 2005. Introduction to statistics through resampling methods and Microsoft Office Excel. John Wiley & Sons.

Grüne, L., Pannek, J., 2011. Nonlinear model predictive control: Theory and algorithms. Springer, London.

Ljung, L., 1987. System identification: Theory for the user. 1 ed., Prentice-Hall, Inc, Englewood Cliffs, NJ.

Luo, J., Huang, W., Zhang, S., 2015. Energy cost optimal operation of belt conveyors using model predictive control methodology. Journal of Cleaner Production 105, 196–205.

Meyer, E., Craig, I., 2015. Dynamic model for a dense medium drum separator in coal beneficiation. Minerals Engineering 77, 78–85.

Meyer, E.J., 2016. MODELLING AND CONTROL OF COAL PROCESSING PLANTS. Ph.D. thesis. University of Pretoria.

Meyer, E.J., Craig, I.K., 2010. The development of dynamic models for a dense medium separation circuit in coal beneficiation. Minerals Engineering 23, 791–805.

Meyer, E.J., Craig, I.K., 2014. Coal dense medium separation dynamic and steady-state modelling for process control. Minerals Engineering 65, 98–108.

Meyer, E.J., Craig, I.K., Alvarado, V., 2015. Unscented Kalman filter for a coal run-of-mine bin. IFAC-PapersOnLine 48, 189–194.

Muller, C.J., Craig, I.K., 2016. Energy reduction for a dual circuit cooling water system using advanced regulatory control. Applied Energy 171, 287–295.

Numbi, B., Zhang, J., Xia, X., 2014. Optimal energy management for a jaw crushing process in deep mines. Energy 68, 337–348.

Olivier, L.E., Craig, I.K., 2013. Model-plant mismatch detection and model update for a run-of-mine ore milling circuit under model predictive control. Journal of Process Control 23, 100–107.

Qin, S.J., Badgwell, T.A., 2003. A survey of industrial model predictive control technology. Control Engineering Practice 11, 733–764.

Steyn, H., 2014. Comminution and separation plant objectives. Private communication.

Yao, L., Ge, Z., 2018. Variable selection for nonlinear soft sensor development with enhanced binary differential evolution algorithm. Control Engineering Practice 72, 68–82.

Zhang, S., Xia, X., 2010. Optimal control of operation efficiency of belt conveyor systems. Applied Energy 87, 1929–1937.

Zhang, S., Xia, X., 2011. Modeling and energy efficiency optimization of belt conveyors. Applied Energy 88, 3061–3071.